Temperature Dependence of the Minority Carrier Diffusion Length in Single Crystal Methylammonium Lead Triiodide Perovskite Nanowires

John Paulus Francia
2017 Summer Physics REU, University of California, Davis

Hybrid organic inorganic perovskites (HOIPs) have been the subject of considerable research in recent years. Such materials show unusually good electric properties, including long carrier diffusion lengths (L). However, the mechanism responsible for these superior electric properties is unknown. Recently, evidence has been shown that the unexpected electrical characteristics of HOIPs are caused by the formation of large polarons. It is also proposed that the electrical properties of some HOIPs, such as methylammonium lead triiodide ($MAPbI_3$), will worsen below 160 K, as these materials undergo a phase change at this temperature. In order to assess the validity of the large polaron model, the temperature dependence of the minority carrier diffusion length (L_D) in single crystal $MAPbI_3$ nanowires was investigated, as the observation of a decrease in the L_D of $MAPbI_3$ when the material was cooled passed 160 K would support the large polaron model.

The L_D of single crystal $MAPbI_3$ nanowires was directly measured using spatially resolved scanning photocurrent microscopy (SPCM). Measurements were carried out at various temperatures between 300 K and 80 K. The measurements did not reveal any clear temperature dependence of the L_D in $MAPbI_3$ nanowires abovr 140 K, only a week dependence below 140 K. However, only a small number of measurements were made. Therefore, these results should be regarded as only preliminary.

In recent years hybrid organic-inorganic perovskites (HOIPs), such as methylammonium lead triiodide ($MAPbI_3$), have emerged as promising photoelectric materials, especially for the production of solar cells. The power conversion efficiency of perovskite based solar cells has increased rapidly in recent years, going from just 3% to 20% in five years [7]. Furthermore, while there is a theoretical limit on the power conversion efficiency of conventional single layer solar cells of about 31%, it has been proposed that single layer solar cells made from HOIPs could achieve a power conversion efficiency as high as 66%[8].

HOIPs are generally solution processed at room temperature. However, solution processed crystals have unavoidable defects which tend to adversely affect their electrical properties. Despite the defects inherent to their production, HOIPs show characteristics of defect free, nonpolar, inorganic semiconductors. They have long carrier diffusion lengths ($L > 100\mu m$), long carrier lifetimes ($\tau > 1\mu s$), and low electron hole recombination rate constants (on the order of $10^{-10}\frac{cm^3}{s}$). This is despite the fact that they have a modest carrier mobility ($\mu \sim 1 - 100\frac{cm^2}{Vs}$) [8].

However, the cause of the unexpected electrical properties of HOIPs is unknown, and is still the subject of debate. While several mechanisms that account for the long τ and L in HOIPs have been proposed, recent evidence shows that these unusually properties are due to the formation of large polarons [8]. A large polaron is a pseudo particle that consists of a charge carrier and the long range lattice deformation that surrounds it. Large polarons only form in highly polar or ionic crystals. A large polaron is created when the lattice near a charge carrier deformed in order to minimize the Coulomb potential between it and the charge carrier. Large polarons have the property of shielding charge carriers from Coulomb interactions with the rest of the lattice. Because of this, they decrease the occurrence of charge carriers becoming trapped, bimolecular recombinations, as well as the cooling of carriers due to scattering with longitudinal optical phonons; thus, accounting for the unexpected electronic properties of HOIPs [8].

$MAPbI_3$ has a perovskite-type structure. It consists of a lead triiodide (PbI_3^-) sub lattice which surrounds a methylammonium (MA^+) cation [1]. A depiction of the crystalline structure of $MAPbI_3$ is shown in **Figure 1**.

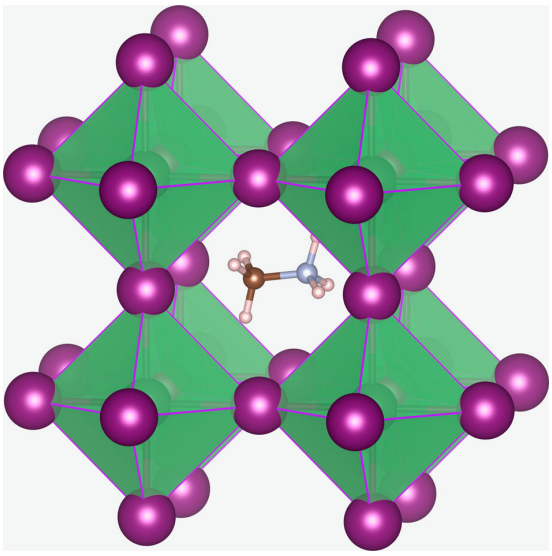

FIG. 1: A depiction of the crystalline structure of $MAPbI_3$ perovskite. Credit for this image is given to: [1]

It has been proposed that the lattice deformation that leads to the formation of large polarons in $MAPbI_3$ stems from two factors. 1) The deformation of the (PbI_3^-) sub lattice and 2) the rotation of the (MA^+) cations. While the PbI_3^- sublattice deforms to minimize the Coulomb potential between it and the charge carriers, the MA^+ cations have rotational freedom at room temperature and thus, can reorient themselves to minimize the Coulomb potential between themselves and the

charge carriers. Due to their rotational freedom, the reorientation of the MA^+ cations is similar to the solvation of an ion in solution and happens on a timescale less than half as large as that of the deformation of the PbI_3^- sublattice [8].

However, $MAPbI_3$ undergoes a phase change at 160 K. Its unit cell is tetragonal above 160 K and orthorhombic below 160 K [5]. It has been proposed that the rotational freedom of the MA^+ cations is frozen out at this tetragonal to orthorhombic phase change, and the rapid liquid like solvation of the charge carriers caused by the rotation of the MA^+ cations no longer contributes to the stabilization of the charge carriers. The formation of the large polarons then happens on the time scale of the PbI_3^- sublattice deformation rather than that of the faster reorientation of the MA^+ cations. Therefore, after the phase change the large polarons will shield the charge carriers less effectively and the carrier lifetime and diffusion length will decrease [8].

In order to cast some light on the validity of the large polaron model, the temperature dependence of the minority carrier diffusion length (L_D) in $MAPbI_3$ was investigated. The L_D in single crystal $MAPbI_3$ nanowires was directly measured by spatially resolved scanning photocurrent microscopy (SPCM) at a range of temperatures.

Transmission electron microscopy performed on similar $MAPbI_3$ nanowires showed that the nanowires were single crystalline [7].

Nanowire devices were made by mechanically transferring $MAPbI_3$ nanowires onto prepatterned gold electrodes, using microfibers. The gap between the electrodes ranged from 8 μm to 20 μm and the nanowires were up to 50 μm in length. **Figure 2** depicts a typical device. Nanowire devices are commonly manufactured using lithographic methods which require e-beam or UV radiation, as well as lift off in polar solvent. However, such methods are not feasible in the production of $MAPbI_3$ devices because $MAPbI_3$ is sensitive to both heat and polar solvents [7]. Kelvin probe force

FIG. 2: 100X magnification of a typical $MAPbI_3$ device. The small gap between the electrodes is close to $8\mu m$ in length and the large gaps are close to $20\mu m$ in length.

microscopy performed on similar devices revealed that Schottky junctions were formed at the nanowire-electrode contacts [7]. The presence of at least one Schottky junction is critical to the extraction of the L_D using SPCM [2].

In a typical SPCM set up (**Figure 3**), a focused laser beam is raster scanned over the device being measured. The current generated through the device as well as the intensity of the light reflected from it are recorded as a function of laser position [2]. $MAPbI_3$ is insulating in the dark, but conducting when exposed to light [7]. When the laser is incident on the $MAPbI_3$ device, charge carriers are generated. Some of the photogenerated charge carriers will reach the electrodes before recombining, resulting in a current [2].

In the relevant experiments, a bias was applied to the electrodes to create stronger band bending at the contacts, which improved charge separation, thus increasing the photocurrent signal [7].

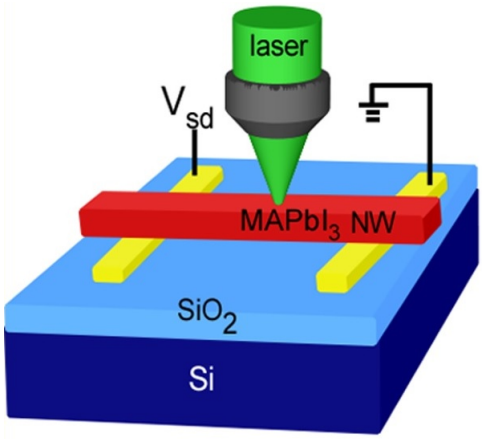

FIG. 3: A depiction of the SPCM setup used in this experiment. Credit for this image is given to: [7]

In order to extract the L_D, the section of the nanowire that extended out of the electrodes was purposefully left long. This was because the electric field was expected to be zero in this region [7]. Because the section of the nanowire that extended out of the electrodes was field free, and the devices contained Schottky junctions at the contacts, the current in the region outside of the electrode was dominated by minority carrier diffusion [2], [7]. Thus, the total current in the region outside of the electrodes was given by $I(x) = Ae^{\frac{-(x-x_0)}{L_d}}$, the minority carrier diffusion current [3]. A is the current near the electrode, x_0 is the position just outside the electrode and x is position. This equation only held for the section of the nanowire that extended out of the electrodes near the minority carrier collection electrode. This was because minority carriers generated on the other side of the electrodes had to cross the gap between the electrodes where a non-zero electric field was present, which complicated the current signal [7].

SPCM generates a 2D photocurrent map of the device being measured (**Figure 4**). It also generates a 2D graph that maps the intensity of the light reflected from the device to the location of the laser (**Figure 5**). This allows one to map a point on the photocurrent map to a position on the device being measured.

A single line was chosen from the 2D photocurrent map. This line graph showed the current as a function of

laser position. By fitting the equation for the current density to the part of the line graph near the electrode with the strongest band bending (the minority carrier collection site), the L_D was extracted.

Figure 6 shows a line graph taken from the photocurrent map shown in **Figure 4** with the minority carrier diffusion current equation fit to it.

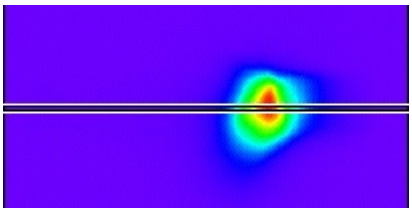

FIG. 4: A 2D photocurrent map of a $MAPbI_3$ device generated by SPCM.

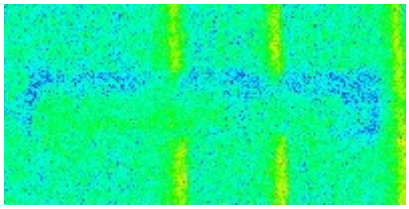

FIG. 5: A reflection image of a $MAPbI_3$ device generated by SPCM.

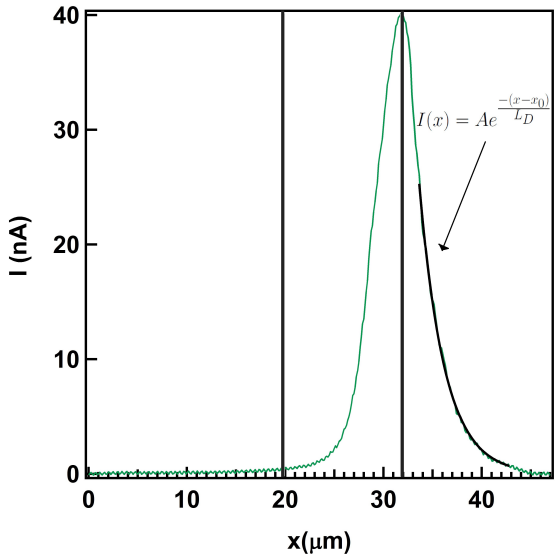

FIG. 6: This graph shows the highlighted cross section of the 2D photocurrent map shown in Figure 2. It shows current density as a function of laser position. The black curve is the current density function fit to the graph with the L_D as the free parameter. The black bars represent the position of the electrodes.

The cryostat used was capable of reaching liquid nitrogen temperatures ($\sim$ 77 K). SPCM measurements were taken at various temperatures between 300 K and 80 K. The temperature of the cryostat was changed at about 4 K per minute. The temperature was keep constant for 10 minutes before each measurement to ensure that the temperature of the device had reached equilibrium. The wavelength of the laser used was $\lambda = 532nm$. The power of the incident laser beam was $\sim 60nW$ and its diameter was $\sim 250nm$. Measurements were taken at each temperature twice, once while decreasing the temperature to 80 K and again while increasing the temperature to 300 K. This was done in order to observe whether any changes in the photocurrent due to temperature were reversible.

Figure 7 and **Figure 8** show SPCM data taken at several temperatures between 300 K and 80 K. **Figure 7** shows data taken while the device was being cooled from 300 K to 80 K and **Figure 8** shows data taken while the device was being warmed from 80 K to 300 K. A positive source-drain bias was applied across the electrodes in both scenarios. It was expected that the current would be the largest near the electrode that collected the minority carriers [7]. Thus, the device appeared to be p-type. When the polarity of the source-drain bias was flipped to that opposite of **Figure 7** and **Figure 8**, the section of the nanowire extending out of the the electrodes near the minority carrier collecting electrode was very short: shorter than the L_D. Thus, this section could not be used to extract the L_D, as the field free section of the nanowire was required to be longer than the L_D for accurate measurements [2].

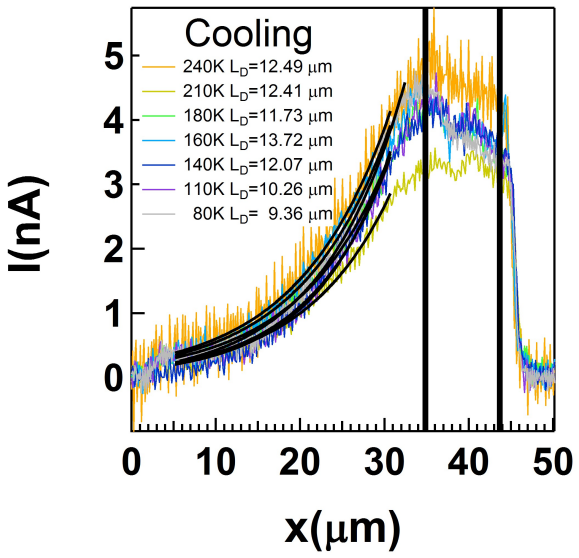

FIG. 7: This graph shows SPCM data taken at several temperatures between 300 K and 80 K while the device being measured was cooled to 80 K. The black curves show the fitting of the minority carrier diffusion current equation. The black bars represent the positions of the electrodes. A source-drain bias of +4 volts was applied across the electrodes. The left electrode was grounded.

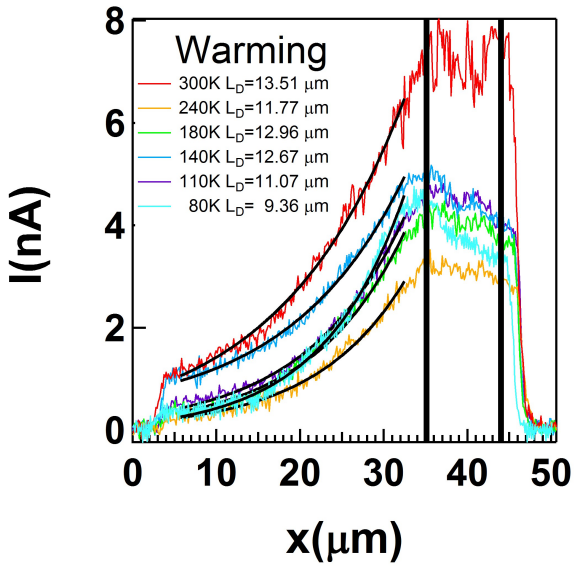

FIG. 8: This graph shows SPCM data taken at several temperatures between 300 K and 80 K while the device being measured was warmed to 300 K. The black curves show the fitting of the minority carrier diffusion current equation. The black bars represent the positions of the electrodes. A source-drain bias of +4 volts was applied across the electrodes. The left electrode was grounded.

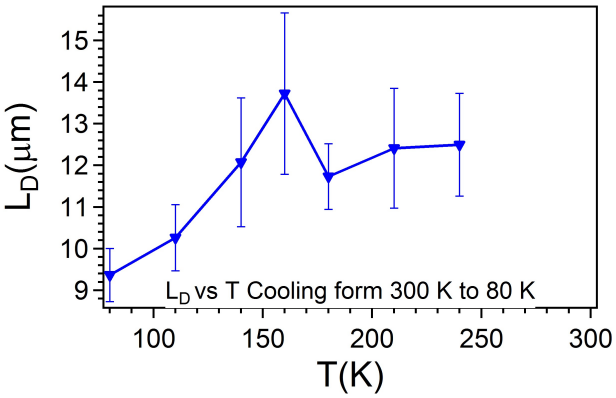

FIG. 9: This graph shows the L_D plotted vs temperature. The data were taken while cooling the device to 80 K. The minority carrier diffusion equation was fit to each curve in several different length regimes. The average of the resulting values for the L_D is shown. The error bars show the standard deviation between these values.

Figure 9 and **Figure 10** show the L_D of a single nanowire device plotted versus temperature. **Figure 9** shows data taken while the device was being cooled and **Figure 10** shows data taken while the device was being warmed. These plots were made using the data shown in **Figure 7** and **Figure 8**. The data point for T = 300 K in **Figure 9** is missing because the phocurrent map generated at that temperature was unclear. Also, fewer measurements were made when warming the device than when cooling the device. These graphs reveal very little change in the L_D as a function of temperature above 140 K, and only a small chance below 140 K. While it is expected that the L_D will change as a function of temperature, a prediction for the temperature dependence - other than a drop in the L_D upon cooling past 160 K - has not been made. The L_D is given by $L_D = \sqrt{D\tau}$, where $D = \mu\frac{kT}{q}$ by the Einstein relationship. However, τ (the charge carrier lifetime) is also dependent on temperature, among other things. Additionally, τ can not be calculated from known quantities and must be determined for a given semiconductor sample by measurements. Because of this, a prediction for the general temperature dependence of L_D can not be made easily. In the above equations D is the diffusion coefficient, μ is the carrier mobility, k is the Boltzmann constant, T is temperature and q is the elementary charge [3], [6], [4]. It is also noteworthy that the data do not show a sudden drop in the L_D at 160 K, where the large polaron model predicts that the L_D will decrease due to the freezing out of the rotational freedom of the MA^+ cation. Additionally, the temperature dependence of the L_D is very similar in measurements made while cooling and warming the device. This suggests that the cause of the change in the L_D as a function of temperature is reversible.

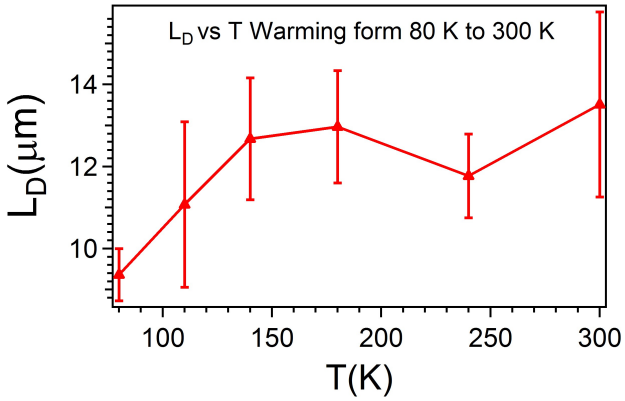

FIG. 10: This graph shows the L_D plotted vs temperature. The data were taken while warming the device to 300 K. The minority carrier diffusion equation was fit to each curve in several different length regimes. The average of the resulting values for the L_D is shown. The error bars show the standard deviation between these values.

However, thus far data have only been gathered from two devices. Therefore, these results should be regarded as preliminary. While these results seem to contradict the large polaron model, it is necessary to conduct more measurements on more devices in order to insure that the data are accurate.

Several experimental difficulties have thus far limited the amount of data gathered. Nanowire transfer took anywhere between several minutes and several hours, as the mechanical transfer of nanowires using microfibers was not very precise: some luck was involved in the placement of the nanowires. Also, less than half of the devices that were manufactured were found to be conductive. This may have been due to the fact that not all of the electrodes that were

made were sufficiently flat. Some had high edges in places. Therefore, there may have been insufficient contact between the nanowires and the electrodes to allow for current to flow. The devices also had a short lifetime.

Since $MAPbI_3$ is sensitive to polar solvents, it will react with the H_2O in the ambient atmosphere, and while the lifetime of the material is extended when it is stored in a nitrogen glove-box, $MAPbI_3$ will degrade within days when left in the open air [7]. However, if a device comes into contact with an excessive amount of H_2O, it will decay within moments.

Experimental difficulties notwithstanding, single crystalline $MAPbI_3$ nanowires were transferred to preprepared electrodes. The L_D of the nanowires was directly measured using SPCM at various temperatures between 300 K and 80 K. The data gathered thus far show no significant change in the L_D as a function of temperature, except for a small decrease in the L_D below 140 K. Additionally, these results seem to contradict the large polaron model, as no dramatic change in the L_D was observed at 160 K. However, these results are only preliminary and more measurements should be made before any conclusion is drawn from them.

[1] Eames, C., Frost, J., Barnes, Piers, B., o'Regan, B., Walsh, A., Islam, S., "Ionic transport in hybrid lead iodide perovskite solar cells," *Nature Communications* **6**, 7497 (2015).

[2] Graham, R., Miller, C., Triplett, M., Yu, D., "Scanning photocurrent microscopy in single nanowire devices," *Proc. of SPIE* **8106**, 81060K (2011).

[3] Graham, R., Yu, D., "Scanning photocurrent microscopy in semiconductor nanostructures" *Modern Physics Letters B* **27**, 1330018 (2013).

[4] Klaassen, M., "A unified mobility model for device simulation–II. Temperature dependence of carrier mobility and lifetime" *Solid-State Electronics* **35**, 961-967 (1992).

[5] Milot, R., Eperon, G., Snaith, H., Johnson, M., Herz, L., "Temperature-dependent charge-carrier dynamics in CH3NH3PbI3 perovskite thin films," *Advanced Functional Materials* **25**, 62186227 (2015).

[6] Pierret,R., "Volume 1 Semiconductor Fundimentals Second Edition," *Addison-Wesley Publishing Company*, 61 (1989).

[7] Xiao, R., Hou, Y., Fu, Y., Peng, X., Wang, Q., Gonzalez, E., Jin, S., Yu, D., "Photocurrent mapping in single-crystal methylammonium lead iodide perovskite nanostructures," *Nano Letters* **16 (12)**, 7710-7717 (2016).

[8] Zhu1, H., Miyata1, K., Fu, Y., Wang1, J., Joshi1, P., Niesner1, Williams, K., Jin, S., Zhu, X.-Y., "Screening in crystalline liquids protects energetic carriers in hybrid perovskites," *Science* **353**, 1409-1413 (2016).